Modeling disinfection and by-product formation during the initial and the second phase of natural water ozonation in a pilot-scale plug flow reactor

A. W. C. van der Helm, L. C. Rietveld, E. T. Baars, P. W. M. H. Smeets and J. C. van Dijk

ABSTRACT

Ozonation experiments (2.5–5 $m^3 h^{-1}$) were performed by dosing dissolved ozone in a continuous flow pilot-scale contactor consisting of a pipe with plug flow reactor (PFR) characteristics. In the PFR ozone, *E. coli*, bromate and AOC concentrations were measured from 1.3 to 1,460 seconds retention time during ozonation of natural water. The experimental data were used to develop an integrated semi-empirical dynamic model describing the measured parameters for the initial phase ($t < \sim 20$ seconds) as well as the second phase ($t > \sim 20$ seconds) of ozone decomposition. It was concluded that for the natural water tested *E. coli* inactivation was very fast, more than 4 log units after 5 seconds for ozone dosages higher than approximately 0.6 mg-$O_3 l^{-1}$. Further it was concluded that semi-empirical models are suited for modeling of ozone decomposition, disinfection, bromate and AOC formation in natural water.

Key words | AOC, bromate, CT, *Escherichia coli* (*E. coli*), model, ozone

A. W. C. van der Helm (corresponding author)
DHV BV, PO Box 1132, 3800 BC Amersfoort,
The Netherlands
Tel.: +31 6 15093313
Fax: +31 33 4682801
E-mail: *alex.vanderhelm@dhv.com*

L. C. Rietveld
J. C. van Dijk
Delft University of Technology,
Sanitary Engineering,
PO Box 5048, 2600 GA Delft,
The Netherlands

E. T. Baars
Waternet,
PO Box 94370, 1090 GJ Amsterdam,
The Netherlands

P. W. M. H. Smeets
Kiwa Water Research,
PO Box 1072, 3430 BB Nieuwegein,
The Netherlands

NOMENCLATURE

AOC	assimilable organic carbon
DOC	dissolved organic carbon
DOPFR	dissolved ozone plug flow reactor
E. coli	*Escherichia coli*
NOM	natural organic matter
PFR	plug flow reactor
UVA_{254}	UV absorbance at 254 nm
Waternet	water cycle company for Amsterdam and surrounding areas
c_{AOC}	AOC concentration ($\mu g\text{-}Cl^{-1}$)
$c_{AOC,in}$	influent AOC concentration ($\mu g\text{-}Cl^{-1}$)
$c_{Br,in}$	influent bromide concentration ($\mu g\text{-}Brl^{-1}$)
c_{BrO_3}	bromate concentration ($\mu g\text{-}BrO_3 l^{-1}$)
$c_{BrO_3,in}$	influent bromate concentration ($\mu g\text{-}BrO_3 l^{-1}$)
$c_{BrO_3,ini}$	initial bromate formation ($\mu g\text{-}BrO_3 l^{-1}$)
$c_{DOC,in}$	influent dissolved organic carbon concentration ($mg\text{-}Cl^{-1}$)
c_{O_3}	concentration of ozone in water ($mg\text{-}O_3 l^{-1}$)
$c_{O_3,DOS}$	ozone dosage ($mg\text{-}O_3 l^{-1}$)
CT	ozone exposure ($(mg\text{-}O_3 l^{-1}) * min$)
CT_{lag}	minimum CT required for obtaining disinfection ($(mg\text{-}O_3 l^{-1}) * min$)
F_{AOC}	constant for AOC formation per DOC ($(\mu g\text{-}Cl^{-1})/(mg\text{-}O_3 l^{-1} * mg\text{-}Cl^{-1})$)
$F_{BrO_3,ini}$	constant for initial bromate formation ($(\mu g\text{-}BrO_3 l^{-1})/(mg\text{-}O_3 l^{-1})$)
k_{10}	inactivation rate constant on a $\log_{10}$ base ($l(mg\text{-}O_3 * min)^{-1}$ for $n = 1$ and $m = 1$)
k_e	inactivation rate constant on a lognormal base ($l(mg\text{-}O_3 * min)^{-1}$)

doi: 10.2166/aqua.2008.089

k_{BrO_3}	bromate formation rate constant $((\mu g\text{-}BrO_3 l^{-1})/((mg\text{-}O_3 l^{-1}) * min))$
k_{O_3}	first-order ozone decomposition rate (s^{-1})
k_{O_3R}	first-order initial ozone decomposition rate (s^{-1})
k_{UVA}	UVA_{254} decay rate (s^{-1})
n, m	empirical constants (−)
n_{CSTR}	number of completely stirred tank reactors (−)
N	number concentration of organisms $(CFU(100\,ml)^{-1})$
N_0	number concentration of organisms at time 0 $(CFU(100\,ml)^{-1})$
N_1/N_0	extrapolated intercept of the first-order line with the ordinate (−)
pH_{in}	influent pH
t	time (s)
T	temperature of the water (°C)
UVA	UVA_{254} in water (m^{-1})
UVA_0	stable UVA_{254} after completion of the ozonation process (m^{-1})
UVA_{in}	influent UVA_{254} (m^{-1})
Y	yield for ozone consumed per UVA_{254} decrease $((mg\text{-}O_3 l^{-1})/(m^{-1}))$
u	water velocity (ms^{-1})
x	length of the reactor (m)

INTRODUCTION

Ozonation is widely used for the treatment of drinking water. It is employed for disinfection, oxidation of micro pollutants, formation of biodegradable organic matter for removal by biological (activated carbon) filtration, and for improvement of color, taste and odor. Ozonation can also be applied in wastewater treatment for oxidation of emerging substances such as endocrine-disrupting chemicals and pharmaceuticals and personal care products (Huber *et al.* 2005). An undesired effect of ozonation in drinking water treatment is the formation of the by-product bromate that is formed in bromide-containing waters (von Gunten 2003).

Ozonation systems usually consist of an ozone dosage section, where gaseous ozone is dissolved in water, and a contactor, for contact time of dissolved ozone. For dosing ozone, different systems can be distinguished. The most applied system is fine bubble diffusion, where ozone gas is added through a number of diffuser plates or a network of perforated pipes in so-called 'bubble chambers'. Bubble chambers can be co-current with water flowing in an upward direction or counter current with water flowing in a downward direction. Bubble chambers can also be applied in series. Other systems for the dosing of ozone are injection with a Venturi mixer (Jackson *et al.* 1999; Rakness 2005), injection just before a static mixer (Chandrakanth *et al.* 2003) or injection in the deep U tube (Roustan *et al.* 1992; Muroyama *et al.* 2005). The ozone contactor after the ozone dosage section usually consists of a number of contact tanks in series, divided by baffles. All these systems applied at full-scale have different hydraulic properties and mixing characteristics. Smeets *et al.* (2006) and van der Helm *et al.* (2007) showed the importance of hydraulic properties and mixing characteristics in bench-scale ozonation experiments with the dosing of dissolved ozone and contact time in a plug flow reactor; the concept was named dissolved ozone plug flow reactor (DOPFR). From these experiments it was concluded that improving plug flow conditions should be considered instead of increasing ozone dosage to improve the disinfection capacity in conventional ozone contactors (Smeets *et al.* 2006).

Ozone is an unstable oxidant in water. In general, when ozone is added to natural water, it decomposes in two phases: the initial phase and the second phase (Buffle *et al.* 2006*a*). The second phase of ozone decomposition (minutes range) follows an empirical first-order rate law, while the initial phase of ozone decomposition (seconds range) follows higher-order kinetics, indicating that other reaction mechanisms take place (Buffle *et al.* 2006*a*). The ozone decomposition in the initial phase is mainly due to reactions with natural organic matter (NOM). As a result of direct ozone consumption by unsaturated bonds in NOM, larger organic components are oxidatively transformed into smaller organic components, and a decrease in UV absorbance at 254 nm (UVA_{254}) occurs. Westerhoff *et al.* (1999) found, from extensive research on physical and chemical properties of NOM isolates, that ozone reacts preferentially with the aromatic constituents of NOM, and specifically activated aromatics. For describing the initial phase, a number of different semi-empirical models can be found in the literature. One group of semi-empirical models consists of a deterministic model for the second phase of ozone decomposition (Staehelin & Hoigné 1982; Bühler

et al. 1984; Staehelin *et al.* 1984) extended with empirical reactions for NOM with ozone and NOM with hydroxyl radicals (Gillogly *et al.* 2001). Another group of semi-empirical models describes the initial phase as an instantaneous ozone demand (Park *et al.* 2001), as a zero-order reaction in the first minute of contact time (Westerhoff *et al.* 1999; Sohn *et al.* 2004) or up to the first 3 minutes of contact time (Gillogly *et al.* 2001), as an instantaneous ozone demand followed by a first-order initial ozone decomposition until approximately 2 minutes of contact time (Westerhoff 2002), and as a function of the decrease in UVA_{254} (Rietveld 2005; van der Helm *et al.* 2007). In the different models the duration of the initial phase of ozone decomposition is different up to a maximum of 3 minutes. Some recent studies on ozone decomposition in the initial phase of ozonation in drinking water and wastewater was done by Buffle & von Gunten (2006) and Buffle *et al.* (2006*a*,*b*) with measurements starting 350 ms after ozone addition. Buffle *et al.* (2006*b*) defined the initial phase of ozone decomposition as the decomposition in the first 20 seconds of contact time ($t < \sim 20$ seconds), and modeled the initial phase as direct reactions between ozone and some highly reactive moieties of the dissolved organic matter. The kinetic model based on parallel bimolecular reactions of reactive moieties with ozone was able to fit the measured ozone decomposition kinetics (Buffle *et al.* 2006*b*).

The objectives of this research are twofold. The first part is assessing different models for the initial ozone decomposition ($t < \sim 20$ seconds), for disinfection, for formation of bromate and for formation of assimilable organic carbon (AOC). The second part is a comparison between ozone decomposition model parameters determined in bench-scale and pilot-scale DOPFR experiments to assess the possibilities for upscaling the DOPFR concept.

MATERIALS AND METHODS

Experimental setup and experiments

Pilot-plant experiments were carried out at Leiduin, one of two drinking water treatment plants of Waternet (water cycle company for Amsterdam and surrounding areas). The water used in the experiments was pre-treated surface water which was infiltrated in the dunes and subsequently treated by aeration and rapid sand filtration. The pilot plant consisted of a DOPFR (see Figure 1).

Ozone was dissolved in a side stream which was pre-treated with reverse osmosis (Hydronautics ESPA2 membrane) for removal of dissolved organic carbon (DOC) and bromide. The dissolved ozone was added to the main stream and mixed in a static mixer. The stainless steel static mixer had an internal diameter of 35 mm, a length of 323 mm and consisted of 4 mixer elements. The total flow

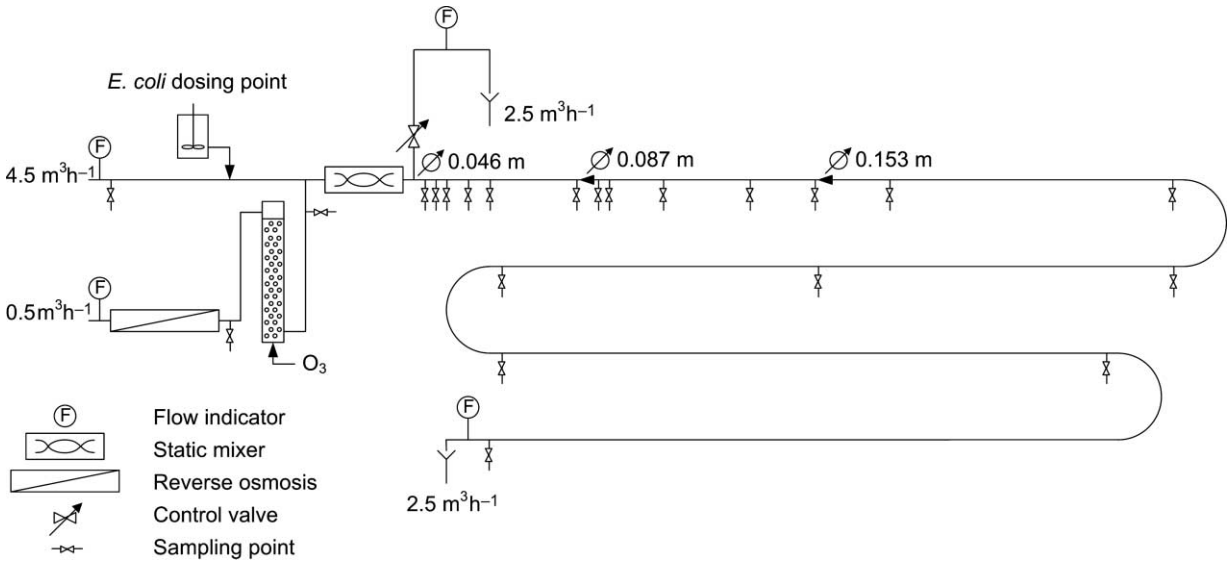

Figure 1 | Experimental setup of the pilot plant.

through the static mixer was 5 m^3h^{-1}, which gave a retention time in the mixer of approximately 0.2 seconds. After the static mixer the water stream was split in two streams of 2.5 m^3h^{-1} each. One stream entered a pipe with the hydraulic properties of a plug flow reactor (PFR), the other stream was not used. According to step-tracer experiments performed in the PFR by Wols *et al.* (2006) the pipe can be modeled as approximately 250 completely mixed tank reactors in series and can thus be seen as a PFR. The pipe starts with a diameter of 0.046 m, after a length of 5 m it changed to 0.087 m and after another length of 5 m it changed to 0.153 m. The total length of the pipe was 63.5 m and it had 19 sampling points, numbered SP1 to SP19. In the installation, the initial phase, as well as the second phase of ozone decomposition was determined simultaneously in one experiment. The retention times at the sampling points SP1 to SP19 were 1.3/1.8/2.3/3.3/4.3/8.3/13.9/15.9/23.5/37.9/48.9/96/248/355/608/829/904/1129/1460 seconds for a flow of 2.5 m^3h^{-1}. In the influent *Escherichia coli* (*E. coli*) were dosed from a vessel with a concentration ranging from 2.2×10^4 to 4.8×10^5 CFUml^{-1}. The ozone dosage is calculated from the measured ozone concentration in the dissolved ozone side stream and the flows of the side stream and the main stream. The calculated ozone dosage is regarded as the ozone concentration in the mixed stream for a retention time of 0 seconds in the PFR just before the static mixer. The pilot plant was operated at low ozone dosages 0.25–1.0 mg-O_3l^{-1} in order to obtain similarities with the full-scale Leiduin treatment plant and to be able to measure *E. coli* at the sampling points. The conditions for the experiments are given in Table 1. The bromate concentration in the influent of the DOPFR (see Table 1) was caused by bromate formation in the bubble column because not all bromide was removed by reverse osmosis. The experimental setup for Experiments 1 to 4 and 9 to 12 differed from data in Figure 1. The flow through the pipe was 5 m^3h^{-1} instead of 2.5 m^3h^{-1} and the first part of the pipe had a diameter of 0.087 m instead of 0.046 m.

The ammonia concentration was always below the detection limit of 0.02 mg-Nl^{-1}. For Experiments 1 to 4, the average temperature was 12.4°C, for Experiments 5 to 8 it was 16.1°C, and for Experiments 9 to 12 it was 18.5°C.

Analytical methods

For Experiments 5 to 8 ozone was analyzed according to the indigo method described by Bader & Hoigné (1982). For Experiments 1 to 4 and 9 to 12, ozone was analyzed according to the DPD method described by Gilbert (1981). Both methods give consistent results (Gilbert & Hoigné 1983). Bromate samples were concentrated on two Ionpac AG9-SC columns and analyzed using a Dionex ICS3000

Table 1 | Conditions and influent water quality parameters for the experiments

		Experiment number											
Parameter	**Unit**	**1**	**2**	**3**	**4**	**5**	**6**	**7**	**8**	**9**	**10**	**11**	**12**
Ozone dosage	mg-O_3l^{-1}	0.37	0.86	0.97	1.91	0.24	0.58	0.77	0.99	0.51	0.69	0.83	1.02
E. coli	CFU/100 ml	–	–	–	–	23,000	13,000	8,200	800	–	–	–	–
pH	–	7.9	7.9	7.9	7.8	8.1	8.0	8.0	8.0	7.9	7.9	7.8	7.8
Bicarbonate	mg-HCO_3l^{-1}	168	164	162	167	169	172	169	170	164	160	162	162
UVA_{254}	m^{-1}	4.7	4.9	4.7	4.9	5.2	5.3	5.2	5.2	5.0	5.0	4.8	4.9
Bromide	μgl^{-1}	147	149	150	147	158*	158*	158*	158*	140	141	142	142
Bromate	$\mu g\text{-}BrO_3l^{-1}$	–	–	–	<0.5	0.6	0.5	0.6	0.6	0.6	0.6	0.6	<0.5
AOC-total	$\mu g\text{-}Cl^{-1}$	7.7	7.8	8.8	7.5	12.6*	12.6*	12.6*	12.6*	8.8†	8.8†	8.8†	11.3
DOC	mg-Cl^{-1}	1.8	2.2	2.1	1.9	1.9	1.8	2.1	2.2	2.0	1.9	1.8	1.7
Temperature	°C	12.6	12.3	12.5	12.0	15.6	16.0	16.7	16.0	18.5	18.4	19.1	17.8

*Measured at experiment 5 and assumed to be constant.
†Measured at experiment 9 and assumed to be constant.

ion chromatograph, with an anion micro membrane suppressor, UV detection (200 nm) and a conductivity meter. Dionex Ionpac AG9-SC, and AS9-SC columns were used with a 0.7 mM $NaHCO_3$ eluent. The detection limit was 0.5 μg-BrO_3l^{-1} (Smeenk *et al.* 1994; Orlandini *et al.* 1997). Bromide samples were analyzed using a Dionex DX120 ion chromatograph, with a chemical suppressor (12.5 mM H_2SO_4), UV detection (200 nm), and a conductivity meter. A Dionex Ionpac AS9-SC column was used with a 0.2 mM $NaHCO_3$/1.4 mM Na_2CO_3 eluent (Orlandini *et al.* 1997). AOC was measured in duplicate, applying the simultaneous incubation of strains P17 and NOX (van der Kooij *et al.* 1982). DOC, pH, bicarbonate and UVA_{254} expressed as the absorbance per metre of cell length were determined using standard procedures (*Standard Methods* 2005). *E. coli* WR1 strain was cultured on a low substrate as described in Smeets *et al.* (2006). Microbiological samples were taken in 1 litre sterile bottles containing sodiumthiosulfate to immediately quench any remaining ozone. Samples were analyzed either by direct filtration and inoculation of the filter or by dilution and direct inoculation of 0.1 ml on agar (Smeets *et al.* 2006).

The CT value for ozonation was determined on the basis of the ozone profile in the PFR determined by the calibrated model:

$$CT = \sum_{i=1}^{n_{CSTR}} c_{O_3,i}{}^{*}(t_i/60 - t_{i-1}/60) \quad (1)$$

where CT is the ozone exposure ((mg-O_3l^{-1}) * min), n_{CSTR} is the number of completely stirred tank reactors (−), c_{O_3} is the concentration of ozone in water (mg-O_3l^{-1}) and t is time (s). In the case of the pilot-scale PFR $n_{CSTR} = 250$.

Initial phase of ozone decomposition

The ozonation model will be used for operational support and for process control with the possibility of on-line calibration and validation. For this purpose, semi-empirical models are most suited. Two different approaches of semi-empirical modeling of ozone decomposition were selected. The description of the initial phase of ozone decomposition by the two approaches was assessed. For the first approach the model of Westerhoff (2002) was selected where the initial phase is modeled as an instantaneous ozone demand followed by first-order ozone decomposition until approximately 2 minutes of contact time:

$$\frac{dc_{O_3}}{dt} = -k_{O_3R}c_{O_3} \quad (2)$$

where k_{O_3R} is the first-order initial ozone decomposition rate (s^{-1}). The amount of ozone consumed during instantaneous ozone demand is determined by the difference in the applied ozone dosage and the intercept of the first-order initial ozone decomposition with the ordinate. Within this approach the model parameters are not related to NOM.

The second approach is an adapted version of the model of Rietveld (2005) and describes the initial phase in relation to NOM by means of the UVA_{254} decrease:

$$\frac{dc_{O_3}}{dt} = -k_{UVA}(UVA - UVA_o)Y \quad (3)$$

$$\frac{d(UVA)}{dt} = -k_{UVA}(UVA - UVA_o) \quad (4)$$

where k_{UVA} is the UVA_{254} decay rate (s^{-1}), UVA is the UVA_{254} in water (m^{-1}), UVA_0 is the stable UVA_{254} after completion of the ozonation process (m^{-1}) and Y is the yield for ozone consumed per UVA_{254} decrease ((mg-O_3l^{-1})/(m^{-1})). This model is calibrated and validated on bench-scale DOPFR (100 lh^{-1}) experiments (van der Helm *et al.* 2007). All model calibrations were performed using linear least squares method. The data used in the model calibrations are the data used to calculate the correlation coefficients.

Disinfection

Disinfection in the pipe was determined by dosing *E. coli* to the tested water and measuring *E. coli* concentration at multiple sampling points in the pipe. The inactivation was modeled using different semi empirical models. Gyürék & Finch (1998) assessed a great number of disinfection models and concluded that the incomplete gamma Hom model, incorporating first-order ozone decomposition, described best the inactivation of heterotrophic plate count bacteria. However, for inactivation models that make use of ozone concentrations calculated by separate equations the incomplete gamma Hom model incorporating

first-order ozone decomposition cannot be used. The Hom model without incorporation of ozone decomposition is given by:

$$\frac{dN}{dt} = -\frac{k_{10}}{60} m N c_{O_3}^{n} t^{m-1} \quad (5)$$

Integration of Equation (5) gives:

$$\log\frac{N}{N_0} = -\frac{k_{10}}{60} c_{O_3}^{n} t^{m} \quad (6)$$

where N is the number concentration of organisms (CFU(100 ml)$^{-1}$), N_0 is the number concentration of organisms at time 0 seconds (CFU(100 ml)$^{-1}$), k_{10} is the inactivation rate constant on a $\log_{10}$ base (l(mg-O_3 * min)$^{-1}$ for $n = 1$ and $m = 1$) and n and m are empirical constants (−). The Hom model is based on the commonly applied semi empirical Chick-Watson model (Hunt & Mariñas 1997; Craik *et al.* 2003; Hijnen *et al.* 2004). The Chick-Watson model describes the rate of disinfection as first-order in time. Hom (1972) introduced the empirical constants n and m after observing that for chlorine disinfection of natural algal-bacterial systems the inactivation was not linear on a log scale but curvilinear. With the Hom model an initial slow inactivation or a tailing-off effect can be described. When $n = 1$ and $m = 1$ the Hom model simplifies to the Chick-Watson model. Haas (1980) theorized an inactivation model and found it was a function of the disinfectant concentration and t^2, so $n = 1$ and $m = 2$.

Another model with slow initial inactivation was described by Rennecker *et al.* (1999). He proposed the delayed Chick-Watson model with a lag-phase for a minimum required ozone dosage:

$$\frac{N}{N_0} = \begin{cases} 1 & \text{if } CT \le CT_{lag} = \frac{1}{k_e}\ln\left(\frac{N_1}{N_0}\right) \\ \frac{N_1}{N_0}\exp(-k_e CT) = \exp(-k_e\{CT - CT_{lag}\}) & \text{if } CT > CT_{lag} = \frac{1}{k_e}\ln\left(\frac{N_1}{N_0}\right) \end{cases} \quad (7)$$

where N_1/N_0 is the extrapolated intercept of the first-order line with the ordinate (−), CT_{lag} is the minimum CT value required for obtaining disinfection ((mg-O_3l^{-1}) * min), and k_e is the inactivation rate constant on a lognormal base (l(mg-O_3 * min)$^{-1}$). The Hom model and the delayed Chick-Watson model were assessed on the experimental data measured in the DOPFR.

Bromate formation

Bromate was measured at multiple sampling points in the pipe. For modeling of bromate formation two different empirical models were applied. The first model was a general multiple linear regression model based on a large amount of data from different locations under different conditions from multiple databases (Carlson *et al.* 2001; Sohn *et al.* 2004):

$$c_{BrO_3} = 1.55\times10^{-6} * (c_{DOC,in})^{-1.26} * (pH_{in})^{5.82} * (c_{O_3,DOS})^{1.57} * (c_{Br,in})^{0.73} * (t/60)^{0.28} * (1.035)^{T-20} \quad (8)$$

where c_{BrO_3} is the bromate concentration (μg-BrO_3l^{-1}), $c_{DOC,in}$ is the influent dissolved organic carbon concentration (mg-Cl)$^{-1}$, $1.1 \le c_{DOC,in} \le 8.4$, pH_{in} is the influent pH, $6.5 \le pH_{in} \le 8.5$, $c_{O_3,DOS}$ is the ozone dosage (mg-O_3l^{-1}), $1.1 \le c_{O_3,DOS} \le 10.0$, $c_{Br,in}$ is the influent bromide concentration (μg-Brl^{-1}), $70 \le c_{Br,in} \le 440$, t is time (s), $1 \le t/60 \le 120$ and T is the temperature of the water (°C), $2 \le T \le 24$.

The second model is a regression model dedicated to one treatment plant (van der Helm *et al.* 2007), using the observation that bromate formation consists of an initial fast increase after which the bromate concentration increases linearly with the CT value (von Gunten & Hoigné 1994; von Gunten *et al.* 2001):

$$c_{BrO_3} = c_{BrO_3,ini} + k_{BrO_3} CT \quad (9)$$

$$c_{BrO_3,ini} = F_{BrO_3,ini} c_{O_3,DOS} + c_{BrO_3,in} \quad (10)$$

where $c_{BrO_3,ini}$ is the initial bromate formation (μg-BrO_3l^{-1}), k_{BrO_3} is the bromate formation rate constant ((μg-Br O_3l^{-1})/((mg-O_3l^{-1}) * min)), $F_{BrO_3,ini}$ is the constant for initial bromate formation ((μg-BrO_3l^{-1})/(mg-O_3l^{-1})), and $c_{BrO_3,in}$ is the influent bromate concentration (μg-BrO_3l^{-1}). Both models were assessed on the experimental data measured in the DOPFR. The initial bromate formation is defined as the extrapolated intercept of the linear bromate formation with the ordinate and is therefore assumed to be instantaneous.

AOC formation

The AOC formation was also measured and modeled. Models for AOC formation are usually empirical linear regression models. The model used describes AOC formation per DOC as a function of the ozone dosage (van der Helm 2007), resulting in the following equation:

$$c_{AOC} = F_{AOC} c_{O_3,DOS} c_{DOC,in} + c_{AOC,in} \quad (11)$$

where c_{AOC} is the AOC concentration ($\mu g\text{-}Cl^{-1}$), F_{AOC} is the constant for AOC formation per DOC ($(\mu g\text{-}Cl^{-1})/(mg\text{-}O_3 l^{-1} * mg\text{-}Cl^{-1})$) and $c_{AOC,in}$ is the influent AOC concentration ($\mu g\text{-}Cl^{-1}$).

Comparison between model parameters determined in bench-scale and pilot-scale DOPFR experiments

The initial ozone decomposition described by Equations (3) and (4) was calibrated and validated on bench-scale DOPFR (100 $l h^{-1}$) experiments (van der Helm *et al.* 2007) including the second phase, modeled by first-order kinetics (Hoigné & Bader 1994). Expanding Equation (3) with the first-order second phase gives:

$$\frac{dc_{O_3}}{dt} = -k_{UVA}(UVA - UVA_0)Y - k_{O_3} c_{O_3} \quad (12)$$

where k_{O_3} is the first-order ozone decomposition rate (s^{-1}). The measured ozone profiles and UVA_{254} decreases in the pilot-scale DOPFR Experiments 1 to 12 were fitted to Equation (12) and (4) as described in van der Helm *et al.* (2007). The fitted ozone decomposition model parameters were compared to the model parameters determined in the bench-scale DOPFR to assess the possibilities of upscaling the DOPFR concept.

RESULTS AND DISCUSSION

Initial phase of ozone decomposition

The results of the model calibrations for the two different approaches for modeling the initial phase of ozone decomposition in Experiments 5 to 8 are presented in Figure 2(a) and (b). In the first approach the initial phase is described as an instantaneous ozone demand followed by first-order initial ozone decomposition in the first two minutes of contact time. This approach was not specifically developed for describing the first seconds of ozone decomposition and was based on batch experiments with the first ozone measurement after 30 to 60 seconds. Consequently, it can be observed from Figure 2(a) that this model does not give an accurate description for the first 20 seconds of contact time, the initial phase as defined by Buffle *et al.* (2006*b*). This model was calibrated on SP1 to SP8 (1.3 to 15.9 seconds) for an ozone dosage of 0.24 $mg\text{-}O_3 l^{-1}$ and on SP5 to SP12 (4.3 to 96 seconds) for ozone dosages of 0.58, 0.77 and 0.99 $mg\text{-}O_3 l^{-1}$, only the first 20 seconds of ozone decomposition are shown. The approach where initial ozone decomposition is a

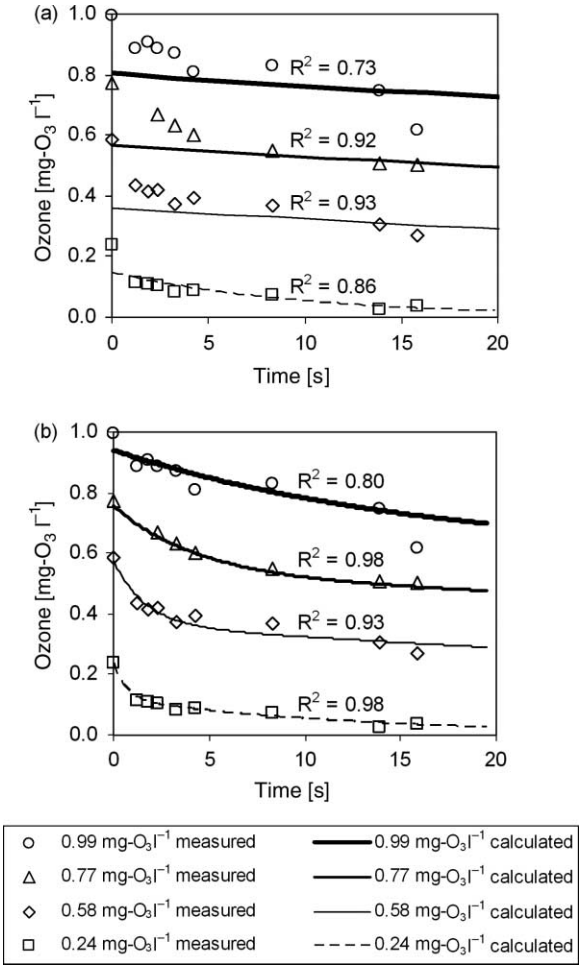

Figure 2 | Initial phase of ozone decomposition for Experiments 5 to 8 modeled by (a) instantaneous ozone demand with first-order initial ozone decomposition and (b) UVA_{254} decrease.

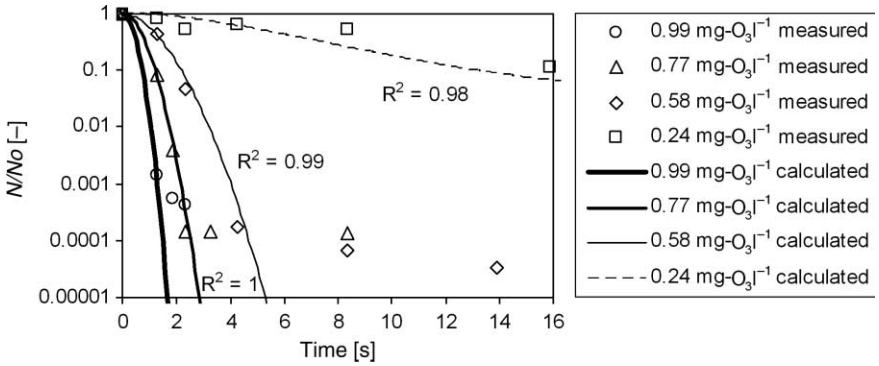

Figure 3 | Modeling inactivation of *E. coli* with the Hom model for Experiments 5 to 8.

function of the UVA_{254} decrease (Figure 2(b)) gives good results for describing the initial phase. This model was calibrated on the ozone dosage ($t = 0$ seconds) and SP1 to SP9 (1.3 to 23.5 seconds); for an ozone dosage of 0.77 mg-O_3l^{-1} the ozone concentrations measured on SP1 and SP2 (1.3 and 1.8 seconds) were not available.

Disinfection

In Experiments 5 to 8 *E. coli* was dosed. The Hom model, Equation (6), and the delayed Chick-Watson model, Equation (7), were fitted to the experimental data. The results are shown in Figures 3 and 4. In accordance with the findings of Haas (1980), best fits with the Hom model were obtained with $n = 1$ and $m = 2$. The inactivation rate constants fitted for the different ozone dosages are presented in Figure 5 and are found to be an exponential function of the ozone dosage:

$$k = 4.49e^{3.305C_{O_3,DOS}} \quad (13)$$

Because k_{10} is calculated for $m = 2$, the unit for k_{10} becomes $l(\text{mg-}O_3 * \text{min})^{-1} * s^{-1}$ (see Equations (5) and (6)). The best results with the delayed Chick-Watson model were achieved with an inactivation rate constant of 316 $l(\text{mg-}O_3 * \text{min})^{-1}$ and CT_{lag} of 0.010 (mg-O_3l^{-1}) * min (Figure 4). For an ozone dosage of 0.58 and 0.77 mg-O_3l^{-1} tailing is observed. For an ozone dosage of 0.24 mg-O_3l^{-1} ozone is depleted before inactivation reaches the point for tailing. For an ozone dosage of 0.99 mg-O_3l^{-1} tailing is assumed to start at an inactivation of approximately 3 log units, however, it is not distinct. Samples that would

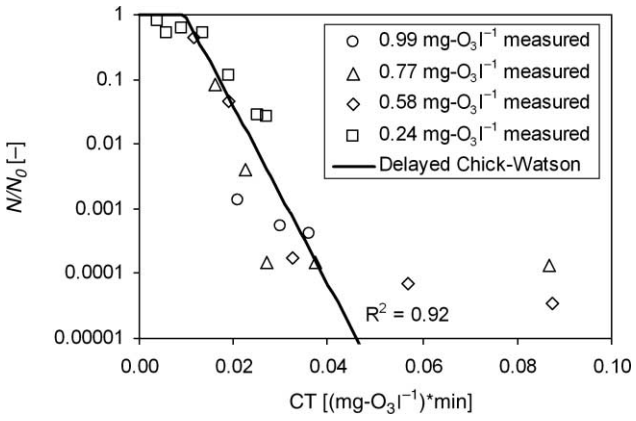

Figure 4 | Modeling inactivation of *E. coli* with the delayed Chick-Watson model for Experiments 5 to 8.

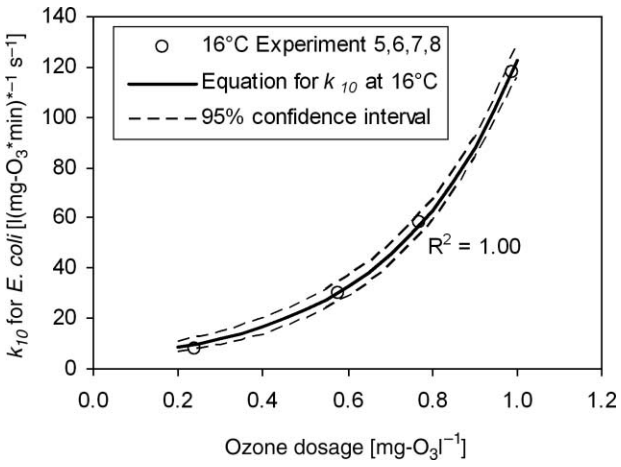

Figure 5 | *E. coli* inactivation rate constants on a $\log_{10}$ base for Hom model, with $n = 1$ and $m = 2$ as a function of the ozone dosage.

correspond to inactivation of more than 4 log units for Experiment 8 with an ozone dosage of 0.99 mg-O_3l^{-1} were all negative due to the low initial *E. coli* concentration of 800 CFU(100 ml)$^{-1}$, so tailing could not be observed.

The model descriptions of both models do not account for tailing, only for the lag phase. This means that the calculated values for *E. coli* inactivation are valid until an inactivation of approximately 4 log units. Figure 3 shows that *E. coli* inactivation is very fast, more than 4 log units after 5 seconds for ozone dosages higher than approximately 0.6 mg-O_3l^{-1}. For the model calibrations in Figure 3 SP1, SP3, SP5, SP6 and SP8 were used for an ozone dosage of 0.24 mg-O_3l^{-1}; SP1, SP3 and SP5 for an ozone dosage of 0.58 mg-O_3l^{-1}; SP1, SP2, SP3 for an ozone dosage of 0.77 mg-O_3l^{-1}; SP1 for an ozone dosage of 0.99 mg-O_3l^{-1}. For the model calibration in Figure 4 all measured *E. coli* data were used for the model calibration until an inactivation of 4 log units.

Bromate formation

Prediction of bromate formation with the multiple linear regression model given by Equation (8) was done for Experiments 5 to 8 (see Figure 6). However, the linear regression model is valid for the ozone dosage range of 1.1 – 10.0 mg-O_3l^{-1}, so it cannot be applied to Experiments 5, 6 and 7, and the correlation coefficient is calculated only for Experiment 8. Bromate formation in the first 60 seconds of contact time was not calculated because the model is only valid after 60 seconds of contact time. Considering the multiple linear regression model is a general model the results for Experiment 8 are quite good. The correlation coefficient for an ozone dosage of 0.99 mg-O_3l^{-1} was determined with data measured at SP12, SP13, SP15 and SP19 for a contact time of 96, 248, 608 and 1,460 seconds, respectively.

Results of modeling bromate formation during the ozonation process in the DOPFR with an initial fast increase followed by a linear increase with the CT value as described by Equations (9) and (10), are shown in Figure 7 for Experiments 5 to 8. For all experiments the bromate formation rate constant used was 1.66 (μg-BrO_3l^{-1})/((mg-O_3l^{-1}) * min) and the constant for initial bromate formation used was 2.17 (μg-BrO_3l^{-1})/(mg-O_3l^{-1}). The constants were calibrated using all measured bromate concentrations as shown in Figure 7, except for concentrations measured at SP1. The usage of the same rate constant gave an overestimation of 30% for Experiment 5, however the absolute overestimation was less than 0.3 μg-BrO_3l^{-1} and the bromate concentrations were very near the detection limit of 0.5 μg- BrO_3l^{-1} (see inset Figure 7).

It can be observed that bromate formation in the pipe modeled as a linear function of the CT value can be applied at low ozone dosages (see Figure 7). However, the correlation is lower for lower ozone dosages.

AOC formation

Results for AOC formation per DOC modeled as a function of the ozone dosage are presented in Figure 8. The constant for AOC formation was 45 (μg-Cl^{-1})/(mg-O_3l^{-1} * mg-Cl^{-1}) for Experiments 5 to 8 at 16.1°C. This regression of AOC formation per DOC as a function of the ozone dosage is

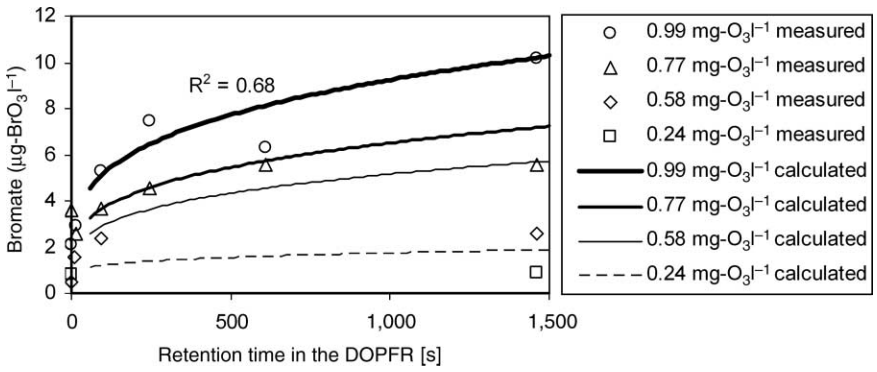

Figure 6 | Bromate formation measured and calculated with the multiple linear regression model for Experiments 5 to 8.

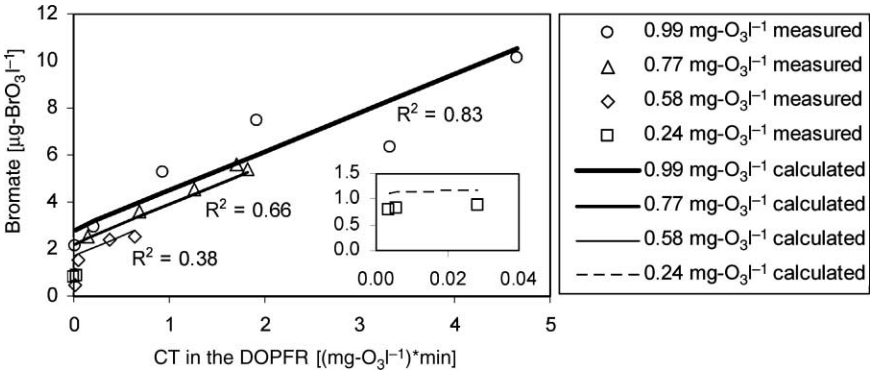

Figure 7 | Bromate formation measured and calculated in the DOPFR, with the model describing bromate formation as an initial fast increase depending on the ozone dosage followed by a linear increase with the CT value for Experiments 5 to 8.

used to give an indication of the AOC formation during ozonation for the natural water tested.

Comparison between model parameters determined in bench-scale and pilot-scale DOPFR experiments

The model given by Equations (12) and (4) has proven to adequately describe ozone decomposition in bench-scale DOPFR (100 l/h) ozonation experiments (van der Helm *et al.* 2007). Some of the data from the bench-scale experiments were used for calibration of the model parameters, k_{O_3}, k_{UVA}, Y and UVA_0, and some for validation of the model. In Figure 9(a)–(d) the calibrated equations for the model parameters based on the bench-scale experiments with their respective confidence intervals are shown. Within these graphs the parameters fitted to the measured ozone concentration profiles and UVA_{254} decreases in the pilot-scale Experiments 1 to 12 are plotted. It is observed that the data from the pilot-scale experiments are within the confidence intervals of the data of the bench-scale experiments for k_{O_3}, k_{UVA} and (UVA_{in} − UVA_0). The values for the Y (Figure 9(c)) are more scattered and partly outside the confidence interval. However, the average of the data including the pilot-scale data gives a horizontal line instead of the increasing line in Figure 9(c). This was to be expected since the yield for consumed ozone per UVA_{254} decrease should be independent of the ozone dosage and the temperature because it has the properties of a stoichiometric coefficient. The k_{O_3} and k_{UVA} are temperature dependent, however, the dependency of k_{O_3} and k_{UVA} on temperature in the pilot-plant experiments is not as pronounced as in the bench-scale experiments. If it is assumed that the model parameters from the bench-scale experiment at 20°C are outliers and taking into account that all pilot-scale experiments with temperatures ranging from 12°C to 19°C are within the confidence intervals determined for 12°C in the bench-scale experiments, no distinction can be made for the model parameters for different

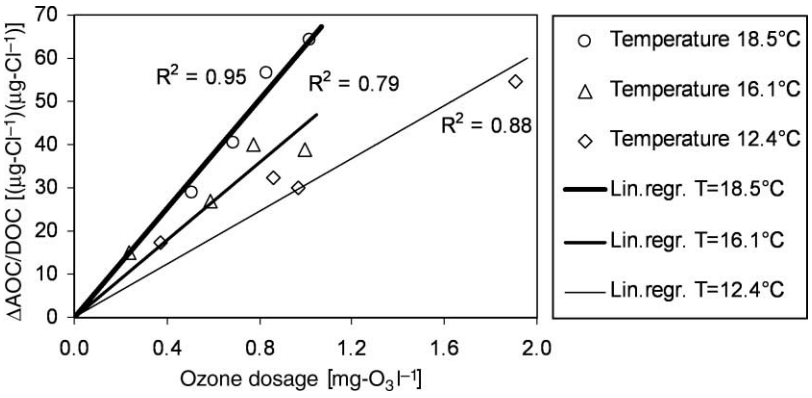

Figure 8 | AOC formation per DOC as a function of the ozone dosage for Experiments 1 to 12.

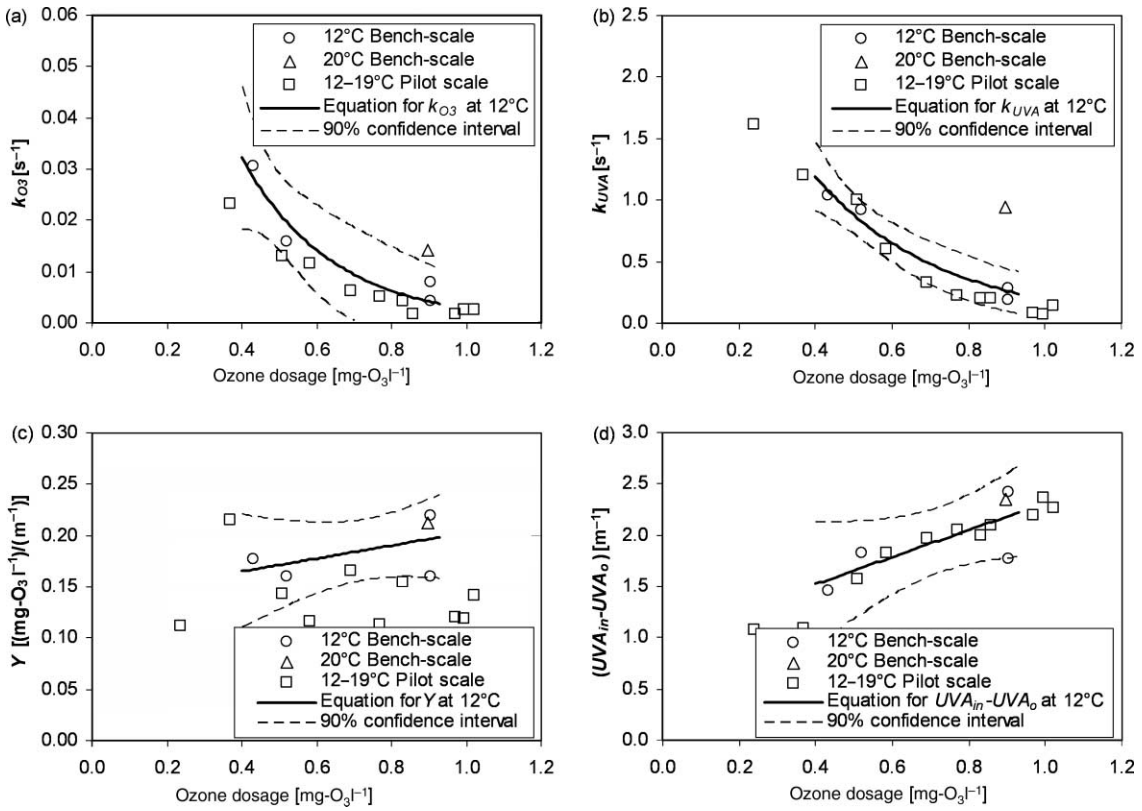

Figure 9 | Comparison between model parameters determined in bench-scale and pilot-scale DOPFR experiments (a) k_{O_3}, (b) k_{UVA}, (c) Y and (d) (UVA_{in} – UVA_0) as a function of the ozone dosage with their 90% confidence intervals for bench-scale experiments (van der Helm *et al.* 2007) and for pilot-scale Experiments 1 to 12.

temperatures based on these experiments. For determination of a temperature dependency a larger number of experiments are needed for a larger temperature range.

In Figure 9(a) there is no value for Experiment 5 with an ozone dosage of 0.24 mg-O$_3$l^{-1} for the first-order ozone decomposition rate in the second phase of ozone decomposition because ozone was depleted after the initial phase. In Figure 9(a) it is observed that the rate of ozone decomposition in the second phase decreased with increasing ozone dosage. Assuming a constant contribution of the ozone decomposition cycle, this can be explained by the various types of sites within NOM that have different reactivity with ozone. For low ozone dosages only the fast-reacting sites consume ozone. When higher ozone dosages were used, the rate of ozone consumption decreased when slowly reacting sites were oxidized as well (Hoigné & Bader 1994; Gallard *et al.* 2003). In Figure 9(b) it is observed that the rate of initial ozone decomposition also decreases with increasing ozone dosage, which was also observed by Buffle *et al.* (2006*b*).

Based on the data from Experiments 1 to 12 with water quality parameters as given in Table 1, the functions for k_{O_3}, k_{UVA}, Y and (UVA_{in} – UVA_0) are:

$$k_{O_3} = 0.1454e^{-4.372C_{O_3,DOS}} \quad (14)$$

$$k_{UVA} = 3.75e^{-3.443C_{O_3,DOS}} \quad (15)$$

$$Y = -0.0042c_{O_3,DOS} + 0.137 \approx 0.137 \quad (16)$$

$$UVA_0 = UVA_{in} - (1.261c_{O_3,DOS} + 1.0237) \quad (17)$$

where UVA_{in} is the influent UVA_{254} (m^{-1}).

Dynamic model for dissolved ozone dosing

In order to simulate the discussed processes simultaneously with regard to changes in the influent water quality over time, the models were incorporated into Stimela (van der Helm & Rietveld 2002). Stimela is an environment where different drinking water treatment processes can

dynamically be modeled. The Stimela models are developed in Matlab/Simulink®. Partial differential equations are numerically integrated to enable the assessment of variations in time and space although the model is calibrated for steady state. For initial ozone decomposition the model using UVA_{254} decrease was used. With this model the initial ozone decomposition is related to reactions with NOM, and with on-line UVA_{254} measurement an extra parameter is available for on-line calibration and validation. To describe disinfection, the Hom model was selected with $n = 1$ and $m = 2$. Reasons for this were its consistency with the inactivation model theorized by Haas (1980) and the fact that it has one parameter less to calibrate than the delayed Chick-Watson model where both k_e and CT_{lag} have to be calibrated. For bromate formation the model based on linearity with CT values was selected because it is able to predict bromate concentrations at low ozone dosages, contrary to the general multiple linear regression model for bromate formation that is not valid for low ozone dosages. Applying bromate formation as a function of the CT value has an extra advantage in a dynamic modeling environment such as Stimela: a partial differential equation for the CT value can be formulated so that the CT development during the ozonation process is simultaneously calculated. Summarizing, the partial differential equations for the ozonation model of the DOPFR were:

$$\frac{\partial c_{O_3}}{\partial t} = -u\frac{\partial c_{O_3}}{\partial x} - k_{UVA}(UVA - UVA_o)Y - k_{O_3}c_{O_3} \tag{18}$$

$$\frac{\partial c_{UVA}}{\partial t} = -u\frac{\partial c_{UVA}}{\partial x} - k_{UVA}(UVA - UVA_o) \tag{19}$$

$$\frac{\partial c_{BrO_3}}{\partial t} = -u\frac{\partial c_{BrO_3}}{\partial x} + k_{BrO_3}c_{O_3}$$
$$c_{BrO_3,ini} = F_{BrO_3,ini}c_{O_3,DOS} + c_{in,BrO_3} \tag{20}$$

$$\frac{\partial N}{\partial t} = -u\frac{\partial N}{\partial x} - k_{10}mNc_{O_3}^{n}(t/60)^{m-1} \tag{21}$$

$$\frac{\partial CT}{\partial t} = -u\frac{\partial CT}{\partial x} + c_{O_3} \tag{22}$$

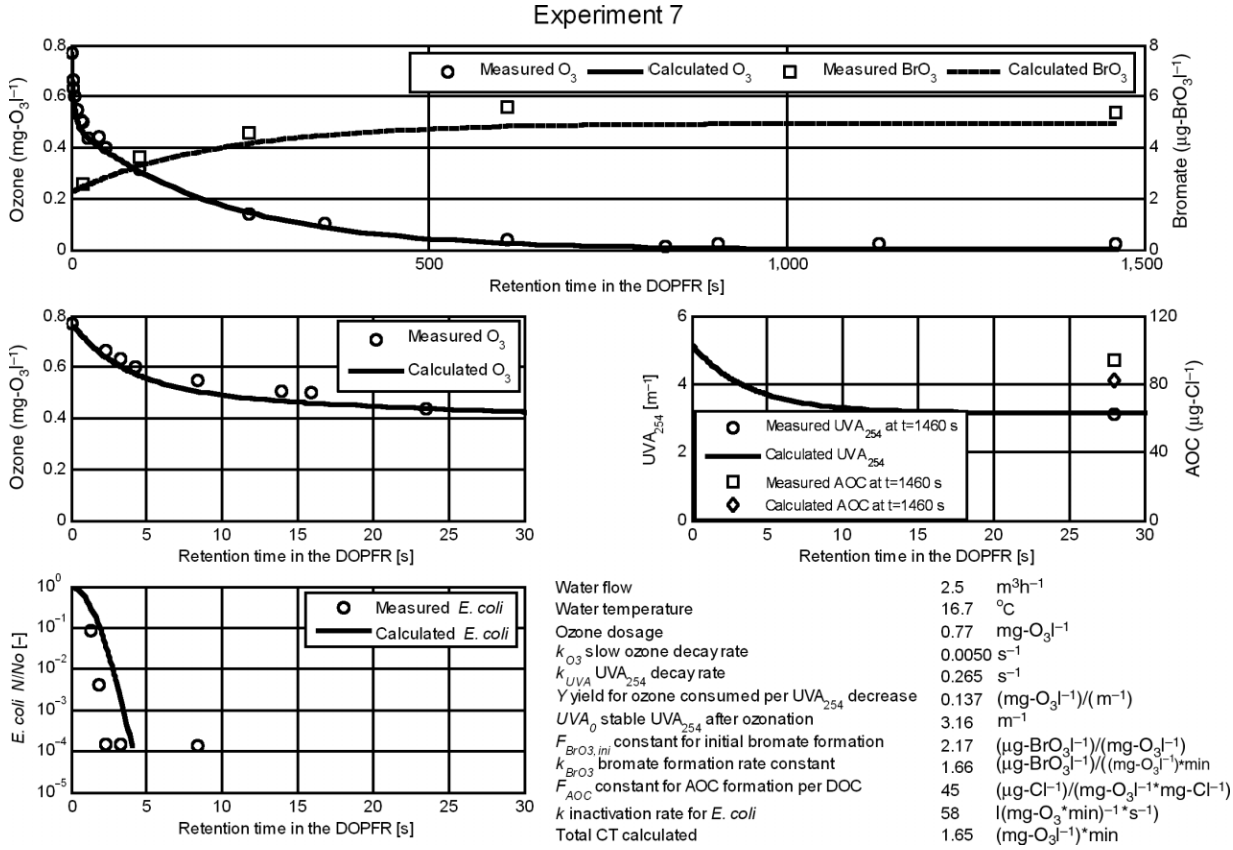

Figure 10 | Results of the dynamic Stimela ozonation model for Experiment 7.

where u is the water velocity (ms^{-1}) and x is the length of the reactor (m). The AOC concentration was not modeled as a partial differential equation but as a regression according to Equation (11). In order to calculate the bromate formation during ozonation the $k_{BrO_3} = 1.66$ ($\mu g\text{-}BrO_3 l^{-1}$)/(($mg\text{-}O_3 l^{-1}$) * min) and $F_{BrO_3,ini} = 2.17$ ($\mu g\text{-}BrO_3 l^{-1}$)/($mg\text{-}O_3 l^{-1}$) were used.

An example of the results of the Stimela ozone model for Experiment 7 is given in Figure 10. All parameters used for the calculations in Figure 10 were determined from the derived relationships. From Figure 10 the differences in time scales for the different processes during ozonation can be observed. It shows that *E. coli* inactivation is 4 log units after 5 seconds, that the major part of the initial ozone decomposition is finished after 20 seconds (UVA_{254} decrease has stopped) and that bromate formation stops after approximately 700 seconds. On the basis of the model calculation, the total CT in the pipe can be accurately estimated and is 1.65 ($mg\text{-}O_3 l^{-1}$) * min. With the model, effects of changes in the operation or changes in the influent water quality can be evaluated. Research is planned for application of the model on different natural waters and extension of the model to incorporate gas exchange in order to model ozone bubble columns. Also research is planned for determining temperature dependencies from new experimental studies and literature, and use of the model for operational support and for process control of ozonation. Validation of the model is planned with data from full-scale conventional ozonation plants.

HO• play an important role during bromate formation. With incorporation of HO• generation in the ozonation model, bromate formation can be predicted more accurately. However, the model was developed for on-line control with possible further on-line calibration. Therefore, the choice was made to discard the involvement of HO• and test whether it was possible to model bromate formation based on just the CT. From these experiments and the experiments described in van der Helm *et al.* (2007) this seems feasible.

CONCLUSIONS

From experiments where ozone decomposition was measured from 1.3 seconds to 1,450 seconds it has been concluded that, for the water tested, a majority of ozone-sensitive organisms were inactivated during the initial phase of ozone decomposition. *E. coli* inactivation of more than 4 log units after 5 seconds was observed for ozone dosages higher than approximately 0.6 $mg\text{-}O_3 l^{-1}$. From comparison of different bromate formation models, it can be concluded that modeling bromate formation as an initial fast increase after which the concentration increases linearly with the CT value gave good results for prediction of bromate formation. From comparison of model parameters for the initial phase ($t < \sim 20$ seconds) as well as the second phase ($t > \sim 20$ seconds) of ozone decomposition based on bench-scale experiments and pilot-scale experiments, it can be concluded that upscaling of the DOPFR concept gives consistent results. Upscaling to a full-scale installation would therefore be possible from the bench-scale and pilot-scale experiments. From pilot-plant experiments an integrated semi-empirical dynamic model was developed for describing ozonation in a DOPFR. It is concluded that semi-empirical models are suited for modeling of ozone decomposition, disinfection, bromate and AOC formation in natural water.

ACKNOWLEDGEMENTS

This research was carried out as part of the project 'Promicit', a cooperation of Waternet, Delft University of Technology, DHV B.V. and ABB B.V. and was subsidized by SenterNovem, Ministry of Economic Affairs, The Netherlands. The aim is to achieve a breakthrough in drinking water quality control by developing an integrated model of the total water treatment and using this model as a basis for operational support and for process control.

REFERENCES

Bader, H. & Hoigné, J. 1982 Determination of ozone in water by the indigo method; a submitted standard method. *Ozone Sci. Eng.* **4**(4), 169–176.

Buffle, M. & von Gunten, U. 2006 Phenols and amine induced HO• generation during the initial phase of natural water ozonation. *Environ. Sci. Technol.* **40**(9), 3057–3063.

Buffle, M., Schumacher, J., Salhi, E., Jekel, M. & von Gunten, U. 2006*a* Measurement of the initial phase of ozone decomposition in water and wastewater by means of a

continuous quench-flow system: application to disinfection and pharmaceutical oxidation. *Water Res.* **40**(9), 1884–1894.

Buffle, M., Schumacher, J., Meylan, S., Jekel, M. & von Gunten, U. 2006*b* Ozonation and advanced oxidation of wastewater: effect of O_3 dose, pH, DOM and HO•-scavengers on ozone decomposition and HO• generation. *Ozone Sci. Eng.* **28**(4), 247–259.

Bühler, R. E., Staehelin, J. & Hoigné, J. 1984 Ozone decomposition in water studied by pulse radiolysis. 1. HO2/O2-and HO3/O3-as intermediates. *J. Phys. Chem.* **88**, 2560–2564.

Carlson, K. H., Bellamy, W., Ducoste, J. & Amy, G. L. 2001 *Implementation of the Integrated Disinfection Design Framework*. AWWARF, Denver, USA.

Chandrakanth, M., Leparc, J., Smith, D. W., Craik, S., Finch, G., Lake, R., Agutter, P., Traversay, C. de, Wolbert, D. & Amy, G. L. 2003 *Improvement of the Ozonation Process through the Use of Static Mixers*. AWWARF/IWA Publishing, London, UK.

Craik, S. A., Smith, D. W., Chandrakanth, M. S. & Belosevic, M. 2003 Efficient inactivation of *Cryptosporidium parvum* in static mixer ozone contactor. *Ozone Sci. Eng.* **25**(4), 295–306.

Gallard, H., von Gunten, U. & Kaiser, H. P. 2003 Prediction of the disinfection and oxidation efficiency of full-scale ozone reactors. *J. Water Supply Res. Technol. AQUA* **52**(4), 277–290.

Gilbert, E. 1981 Photometrische Bestimmung niedriger Ozonkonzentrationen in Wasser mit Hilfe von Diäthyl-p-phenylendiamin (DPD) (Photometric determination of low ozone concentrations in water using Diethyl-p-phenylenediamine (DPD)). *GWF Wasser Abwasser* **122**(9), 410–416.

Gilbert, E. & Hoigné, J. 1983 Messung von Ozon in Wasserwerken; Vergleich der DPD- und Indigo-Methode (Measurement of ozone in water treatment; comparison of the DPD and indigo method). *GWF Wasser Abwasser* **124**(11), 527–531.

Gillogly, T., Najm, I., Minear, R., Mariñas, B., Urban, M., Kim, J. H., Echigo, S., Amy, G., Douvillle, C., Daw, B., Andrews, R., Hofmann, R. & Croué, J. P. 2001 *Bromate Formation and Control during Ozonation of Low Bromide Waters*. AWWARF/AWWA, Denver, USA.

Gyürék, L. L. & Finch, G. R. 1998 Modeling water treatment chemical disinfection kinetics. *J. Environ. Eng.–ASCE* **124**(9), 783–793.

Haas, C. N. 1980 A mechanistic kinetic model for chlorine disinfection. *Environ. Sci. Technol.* **14**(3), 339–340.

Hijnen, W. A. M., Baars, E. T., Bosklopper, Th. G. J., van der Veer, A. J., Meijers, R. T. & Medema, G. J. 2004 Influence of DOC on the inactivation efficiency of ozonation assessed with Clostridium perfringens and a lab-scale continuous flow system. *Ozone Sci. Eng.* **26**(5), 465–473.

Hoigné, J. & Bader, H. 1994 Characterization of water quality criteria for ozonation processes. Part II: lifetime of added ozone. *Ozone Sci. Eng.* **16**(2), 121–134.

Hom, L. W. 1972 Kinetics of chlorine disinfection in an ecosystem. *J. Sanit. Eng. Div.* **98**(SA1), 183–194.

Huber, M. M., Göbel, A., Joss, A., Hermann, N., Löffler, D., McArdell, C. S., Ried, A., Siegrist, H., Ternes, T. A. & von Gunten, U. 2005 Oxidation of pharmaceuticals during ozonation of municipal wastewater effluents: a pilot study. *Environ. Sci. Technol.* **39**(11), 4290–4299.

Hunt, N. K. & Mariñas, B. J. 1997 Kinetics of *Escherichia coli* inactivation with ozone. *Water Res.* **31**(6), 1355–1362.

Jackson, J. R., Overbeck, P. K. & Overby, J. M. 1999 Dissolved oxygen control by pressurized side stream ozone contacting and degassing. *Proceedings of the IOA-EA3G 14th World Congress and Exhibition*, Dearborn, USA, 1999.

Muroyama, K., Yamasaki, M., Shimizu, M., Shibutani, E. & Tsuji, T. 2005 Modeling and scale-up simulation of U-tube ozone oxidation reactor for treating drinking water. *Chem. Eng. Sci.* **60**(22), 6360–6370.

Orlandini, E., Kruithof, J., van der Hoek, J. P., Siebel, M. & Schippers, J. 1997 Impact of ozonation on disinfection and formation of biodegradable organic matter and bromate. *J. Water Supply Res. Technol. AQUA* **46**(1), 20–30.

Park, H., Hwang, T., Kang, J., Choi, H. & Oh, H. 2001 Characterization of raw water for the ozone application measuring ozone consumption rate. *Water Res.* **35**(11), 2607–2614.

Rakness, K. L. 2005 *Ozone in Drinking Water Treatment: Process Design, Operation, and Optimization*. AWWA, Denver, USA.

Rennecker, J. L., Mariñas, B. J., Owens, J. H. & Rice, E. W. 1999 Inactivation of *Cryptosporidium parvum oocysts* with ozone. *Water Res.* **33**(11), 2481–2488.

Rietveld, L. C. 2005 *Improving Operation of Drinking Water Treatment through Modelling*. PhD Thesis, Faculty of Civil Engineering and Geosciences, Delft University of Technology.

Roustan, M., Liné, A. & Wable, O. 1992 Modeling of vertical downward gas-liquid flow for the design of a new contactor. *Chem. Eng. Sci.* **47**(13–14), 3681–3688.

Smeenk, J. G. M. M., van Rossum, W. J. M., Gademan, W. J. H. & Bruggink, C. 1994 Trace level determination of bromate and chlorite in drinking and surface water by ion chromatography with automated preconcentration. *Proceedings of the International Ion Chromatography Symposium*, Torino, Italy, 1994.

Smeets, P. W. M. H., van der Helm, A. W. C., Dullemont, Y. J., Rietveld, L. C., van Dijk, J. C. & Medema, G. J. 2006 Inactivation of *Escherichia coli* by ozone under bench-scale plug flow and full-scale hydraulic conditions. *Water Res.* **40**(17), 3239–3248.

Sohn, J., Amy, G., Cho, J., Lee, Y. & Yoon, Y. 2004 Disinfectant decay and disinfection by-products formation model development: chlorination and ozonation by-products. *Water Res.* **38**(10), 2461–2478.

Staehelin, J. & Hoigné, J. 1982 Decomposition of ozone in water: rate of initiation by hydroxide ions and hydrogen peroxide. *Environ. Sci. Technol.* **16**(10), 676–681.

Staehelin, J., Bühler, R. E. & Hoigné, J. 1984 Ozone decomposition in water studied by pulse radiolysis. 2. OH and HO4 as chain intermediates. *J. Phys. Chem.* **88**(24), 5999–6004.

Standard Methods for the Examination of Water & Wastewater 2005 21st edn, American Public Health Association/American

Water Works Association/Water Environment Federation, Baltimore, USA.

van der Helm, A. W. C. 2007 *Integrated Modeling of Ozonation for Optimization of Drinking Water Treatment*. PhD Thesis, Water Management Academic Press, Delft, the Netherlands.

van der Helm, A. W. C. & Rietveld, L. C. 2002 Modelling of drinking water treatment processes within the Stimela environment. *Water Sci. Technol.: Water Supply* **2**(1), 87–93.

van der Helm, A. W. C., Smeets, P. W. M. H., Baars, E. T., Rietveld, L. C. & van Dijk, J. C. 2007 Modelling of ozonation for dissolved ozone dosing. *Ozone Sci. Eng.* **29**(5), 379–389.

van der Kooij, D., Visser, A. & Hijnen, W. A. M. 1982 Determining the concentration of easily assimilable organic carbon in drinking water. *Am. Water Works Assoc. J.* **74**(10), 540–545.

von Gunten, U. 2003 Ozonation of drinking water: part II. Disinfection and by-product formation in presence of bromide, iodide or chlorine. *Water Res.* **37**(7), 1469–1487.

von Gunten, U. & Hoigné, J. 1994 Bromate formation during ozonation of bromide-containing waters: interaction of ozone and hydroxyl radical reactions. *Environ. Sci. Technol.* **28**(7), 1234–1242.

von Gunten, U., Driedger, A., Gallard, H. & Salhi, E. 2001 By-products formation during drinking water disinfection: a tool to assess disinfection efficiency? *Water Res.* **35**(8), 2095–2099.

Westerhoff, P. 2002 *Kinetic-based Models for Bromate Formation in Natural Waters*. USEPA, Washington, USA.

Westerhoff, P., Aiken, G., Amy, G. & Debroux, J. 1999 Relationships between the structure of natural organic matter and its reactivity towards molecular ozone and hydroxyl radicals. *Water Res.* **33**(10), 2265–2276.

Wols, B. A., Hofman, J. A. H. M., Uijttewaal, W. S. J. & van Dijk, J. C. 2006 The effect of turbulent diffusion on the performance of ozone systems. *Proceedings of the Workshop Developments in Drinking Water Treatment Modelling*, Delft University of Technology, Delft, The Netherlands, 2006.

First received 13 September 2007; accepted in revised form 13 February 2008